Int. Symposium on Applied Machine Intelligence and Informatics, SAMI 2017 IEEE proceedings, pp.431-434,,
ISBN 978-1-8090-5655-2

Spherical RBF Vector Field Interpolation: Experimental Study

Michal Smolik*, Vaclav Skala*
* University of West Bohemia/Faculty of Applied Sciences, Plzen, Czech Republic
smolik@kiv.zcu.cz, www.vaclavskala.eu

***Abstract*—The Radial Basis Function (RBF) interpolation is a common technique for scattered data interpolation. We present and test an approach of RBF interpolation on a sphere which uses the spherical distance on the surface of the sphere instead of the Euclidian distance. We show how the interpolation of vector field data depends on the value of shape parameter of RBF and find the optimal shape parameter for our experiments.**

***Keywords*—Radial basis functions; vector field; interpolation; spherical distance; shape parameter.**

I. INTRODUCTION

Interpolation is frequently applied operation used in computational methods. Several methods have been developed for data interpolation, but they expect some kind of data "ordering", e.g. structured mesh, rectangular mesh, unstructured mesh etc. However, in many engineering problems, data are not ordered and they are scattered in k-dimensional space, in general. Often, in technical applications, the scattered data are tessellated using triangulation but this approach is quite prohibitive for the case of k-dimensional data interpolation because of the computational cost, i.e. if data is large.

Interpolating scattered vector data on a surface becomes frequent in applied problem solutions. When the underlying manifold is a sphere, there are applications to geodesy [1], meteorology [3], astrophysics, geophysics, geosciences [4] and other areas. The radial basis function interpolation on a sphere [5] has the advantage of continuous interpolant all over the sphere, as there are no borders.

II. VECTOR FIELD

Vector fields on surfaces are important objects which appear frequently in scientific simulation in CFD (Computational Fluid Dynamics) [10] or modelling by FEM (Finite Element Method). To be visualized [6], such vector fields are usually linearly approximated for the sake of simplicity and performance considerations.

The vector field can be easily analyzed when having an approximation of the vector field near some location point. The important places to be analyzed are so called critical points. Analyzing the vector field behavior near these points gives us the information about the characteristic of the vector field.

A. Critical Point

Critical points ($\boldsymbol{x}_0$) of the vector field are points where the magnitude of the vector vanishes

$$\frac{d\boldsymbol{x}}{dt} = \boldsymbol{v}(\boldsymbol{x}) = \boldsymbol{0}\,, \tag{1}$$

i.e. all components are equal to zero

$$\begin{bmatrix} \frac{dx}{dt} \\ \frac{dy}{dt} \end{bmatrix} = \begin{bmatrix} 0 \\ 0 \end{bmatrix}. \tag{2}$$

A critical point is said to be isolated, or simple, if the vector field is non-vanishing in an open neighborhood around the critical point. Thus, for all surrounding points $\boldsymbol{x}_\varepsilon$ of the critical point $\boldsymbol{x}_0$ the equation (1) does not apply, i.e.

$$\frac{d\boldsymbol{x}_\varepsilon}{dt} \neq \boldsymbol{0}\,. \tag{3}$$

At critical points, the direction of the field line is indeterminate, and they are the only points in the vector field were field lines, e.g. stream lines in a CFD dataset, can intersect (asymptotically). The terms singular point, null point, neutral point or equilibrium point are also frequently used to describe critical points.

Critical points deliver important information about the overall characteristics of a vector field because together with the nearby surrounding vectors, they have more information encoded in them than any such group in the vector field, regarding the total behavior of the field.

III. VECTOR FIELD INTERPOLATION

The RBF interpolation was originally introduced by [7] and is based on computing the distance of two points in the k-dimensional space and is defined by a function

$$f(\boldsymbol{x}) = \sum_{j=1}^{M} \lambda_j \, \varphi\left(\left\|\boldsymbol{x} - \boldsymbol{x}_j\right\|\right), \tag{4}$$

where λ_j are weights of the RBF, M is number of radial basis functions, i.e. number of reference points, and φ is the radial basis function.

The radial basis function interpolation can be computed on a sphere and has some advantages [2], [8]. There are any unphysical boundaries and there are no problems with interpolation on the poles, i.e. the sphere has no boundaries, and the vector field can be interpolated on the whole sphere surface at once compared to using only spherical coordinates and interpolation in $2D$. The other advantage is that there are no coordinate singularities and the maximal distance of any two points has an upper bound and the RBF interpolation does not need any mesh, i.e. triangulation, for interpolation.

The RBF interpolation interpolates scalar values on a sphere. However the vector field is not a scalar field, the RBF

interpolation can be used for vector fields as well. For each component of the vector, we need to compute one RBF interpolation separately but it should be noted that the interpolation matrices for all component of the vector are the same.

The calculation of the distance r between two points $\boldsymbol{x}_1$ and $\boldsymbol{x}_2$ on a sphere can be computed as the Euclidian distance between this two points

$$r = \|\boldsymbol{x}_1 - \boldsymbol{x}_2\|_{Euclidian} = \sqrt{(\boldsymbol{x}_1 - \boldsymbol{x}_2)^T \cdot (\boldsymbol{x}_1 - \boldsymbol{x}_2)}\,. \tag{5}$$

In the case that both points lie on a unit sphere then $r \in \langle 0; 2\rangle$.

Or the distance can be computed as the shortest distance between two points $\boldsymbol{x}_1$ and $\boldsymbol{x}_2$ on the surface of a sphere, measured along the surface of the sphere. The distance is computed using

$$r = \|\boldsymbol{x}_1 - \boldsymbol{x}_2\|_{spherical} = \cos^{-1}(\boldsymbol{n}_1 \cdot \boldsymbol{n}_2)\,, \tag{6}$$

where $r \in \langle 0; \pi\rangle$ and

$$\boldsymbol{n}_1 = \frac{\boldsymbol{x}_1}{\|\boldsymbol{x}_1\|} \qquad \boldsymbol{n}_2 = \frac{\boldsymbol{x}_2}{\|\boldsymbol{x}_2\|} \tag{7}$$

The distance r in (6) is measured in radians. In the case that the sphere has radius equal to one, the computed distance in radians is equal to the distance measured along the surface of the sphere.

The RBF interpolation performs slightly better interpolation results when using spherical distance (6) compared to the RBF with the Euclidian distance calculation (5). For this reason we use only the spherical distance calculation for all our tests.

IV. RESULTS

For experimental verification of the proposed approach an analytical function is used.

An example of a vector field on a sphere can be described analytically. The analytical function has to fulfill a criterion which is that the function must be continuous all over the sphere including wrapping. For this purpose we can use goniometric functions that have periodicity equal to 2π, i.e. for example a vector field with the following formula

$$\begin{bmatrix} u \\ v \end{bmatrix} = \begin{bmatrix} \sin 3\delta + \cos 4\delta \cdot \cos 3\delta \\ \cos 4\theta - \sin 4\theta \cdot \sin 3\delta \end{bmatrix}, \tag{8}$$

where δ is an azimuth angle, i.e. $\delta \in (-\pi; \pi\rangle$ and θ is a zenith angle, i.e. $\theta \in \langle 0; \pi\rangle$. Vector $[u, v]^T$ represents a directional vector in the spherical coordinates on the surface of a sphere at point $\boldsymbol{P} = [P_x, P_y, P_z]^T$

$$\begin{bmatrix} P_x \\ P_y \\ P_z \end{bmatrix} = \begin{bmatrix} \sin\theta\cos\delta \\ \sin\theta\sin\delta \\ \cos\theta \end{bmatrix}. \tag{9}$$

The vector field (8) was discretized by 10 000 uniformly distributed points on a surface of a sphere and then interpolated using RBF on sphere with Compact-Support-RBFs (CSRBF) [9]

$$\varphi(r) = \begin{cases} (1-\varepsilon r)^4(4\varepsilon r + 1) & \varepsilon r \le 1 \\ 0 & \varepsilon r > 1 \end{cases}, \tag{10}$$

where ε is a shape parameter and r is the distance measured over the surface of a sphere.

We computed the RBF interpolation on a sphere of the original vector field (8) using 10^3, $5 \cdot 10^3$ and 10^4 sampling points for different shape parameters and measured the average vector length error and the average angular displacement error of interpolated vectors. The shape parameter ε cannot be less than $1/\pi$, as the CSRBF with $\varepsilon = 1/\pi$ covers the whole surface of a unit sphere, i.e. the CSRBF with shape parameter $\varepsilon > 1/\pi$ covers only a part of the sphere surface.

The vector length error is computed using the formula

$$err_l = \frac{\sum_{i=1}^{N} |\|\tilde{\boldsymbol{v}}_i\| - \|\boldsymbol{v}_i\||}{\sum_{i=1}^{N} \|\boldsymbol{v}_i\|}, \tag{11}$$

where $\tilde{\boldsymbol{v}}_i$ is the interpolated vector and $\boldsymbol{v}_i$ is the vector computed from the analytical function (8). The vector length error is visualized in Figure 1. It can be seen that the average error is almost identical for shape parameter $\varepsilon \in \langle 1/\pi\,;\, 4\rangle$ for $5 \cdot 10^3$ and 10^4 sampling points and for larger shape parameters the error increases. The vector length error for 10^3 sampling points is slightly higher than for $5 \cdot 10^3$ and 10^4 sampling points and starts distinctly increasing for shape parameter $\varepsilon > 2$.

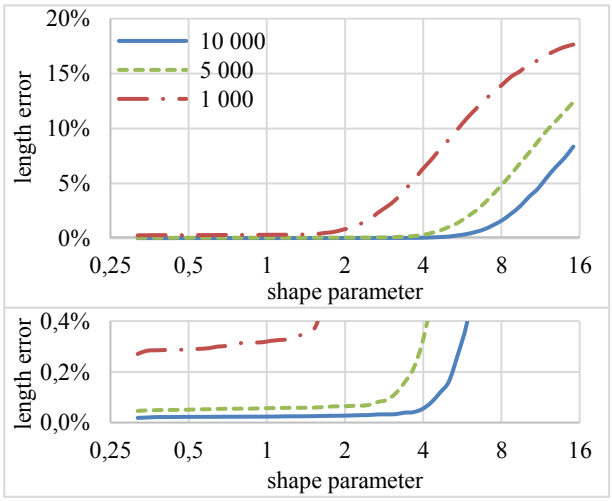

Figure 1: Average error of vector lengths of the RBF interpolation on a sphere for different shape parameters and different numbers of interpolated points.

The average angular displacement error is computed using the formula

$$err_\varphi = \frac{\sum_{i=1}^{N} \cos^{-1}(\tilde{\boldsymbol{v}}_i \cdot \boldsymbol{v}_i)}{N} \cdot \frac{180}{\pi}. \tag{12}$$

The results of the average angular displacement error are visualized in Figure 2. The progress of the error is similar to Figure 1 and, thus, the quality of the vector field interpolation is almost identical for shape parameters $\varepsilon \in \langle 1/\pi\,;\, 4\rangle$ for $5 \cdot 10^3$ and 10^4 sampling points and for larger shape parameters the error increases. The angular displacement error for 10^3

IEEE proceedings, pp.431-434,,
ISBN 978-1-8090-5655-2

sampling points is slightly higher than for $5 \cdot 10^3$ and 10^4 sampling points and starts distinctly increasing for shape parameter $\varepsilon > 2$.

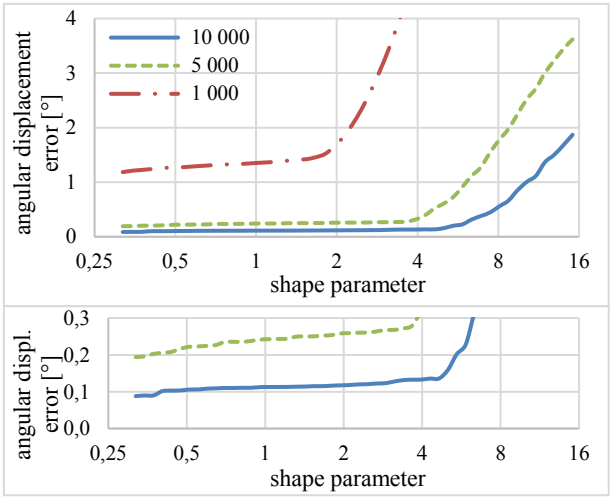

Figure 2: Average angular displacement error [°] of vectors of RBF interpolation on a sphere for different shape parameters and different numbers of interpolated points.

The CSRBF (10) is a "local" radial basis function, therefore, the RBF interpolation matrix is sparse. We varied the shape parameter and measured the occupancy of the interpolation matrix. The results can be seen in Figure 4. When the shape parameter is $\varepsilon > 2/\pi$ then more than half of the elements in the RBF interpolation matrix are equal zero.

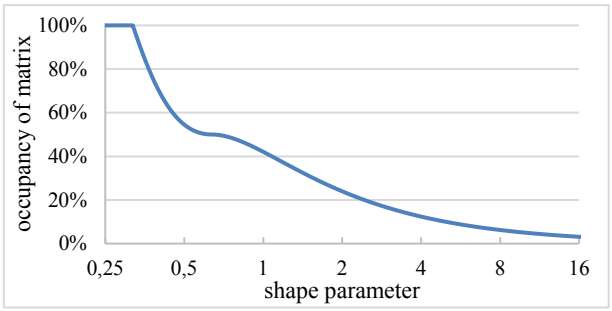

Figure 4: Occupancy of the interpolation matrix for the RBF interpolation on a unit sphere for different shape parameters.

The RBF interpolation matrix has different condition numbers for different shape parameters because the occupancy of the matrix changes for different shape parameters. The condition number of this matrix is visualized in Figure 5 and it can be seen that the matrix is better conditioned with increasing shape parameter. It is justified by the fact that the occupancy of the RBF interpolation matrix decreases for increasing shape parameter.

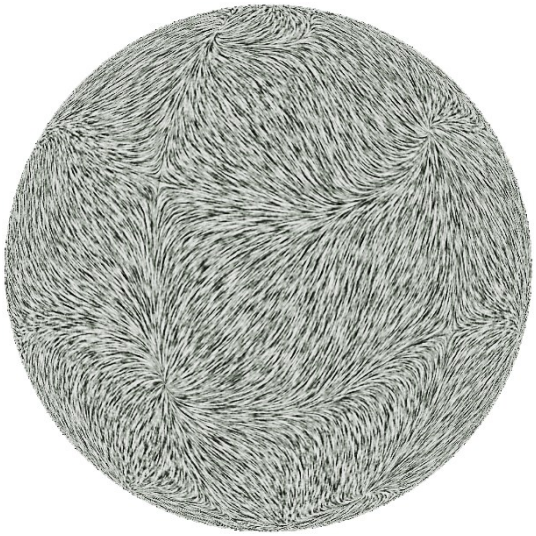

Figure 3: Line integral convolution visualization of the RBF interpolated vector field (8).

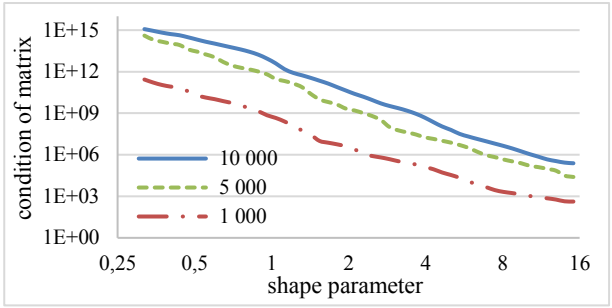

Figure 5: Condition of the RBF interpolation matrix for different shape parameters and different numbers of interpolated points.

We performed another series of tests with a different CSRBF function as well. The second CSRBF used for our tests is

$$\varphi(r) = \begin{cases} (1-\varepsilon r)^3(3\varepsilon r+1) & \varepsilon r \le 1 \\ 0 & \varepsilon r > 1 \end{cases}, \qquad (13)$$

We performed the same tests as for (10). The results of average vector field length error are visualized in the following graph, i.e. Figure **6**.

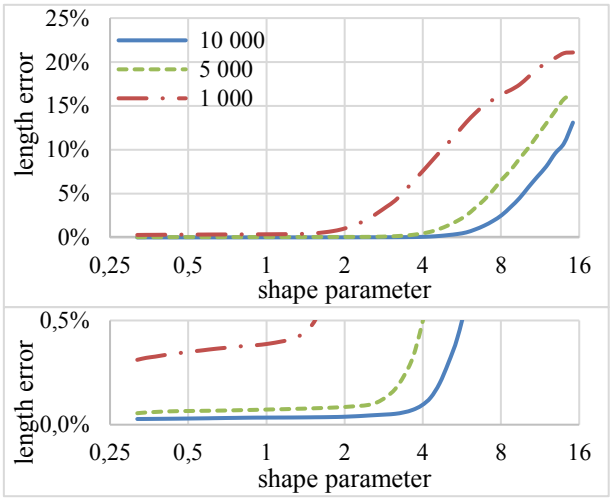

Figure 6: Average error of vector lengths of the RBF interpolation on a sphere for different shape parameters and different numbers of interpolated points.

The results of average angular displacement error are visualized in the following graph, i.e. Figure **7**.

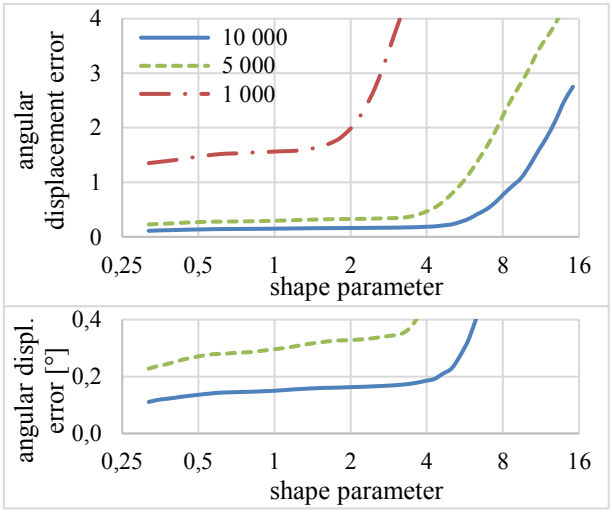

Figure 7: Average angular displacement error [°] of vectors of RBF interpolation on a sphere for different shape parameters and different numbers of interpolated points.

It can be seen, that the results for both CSRBF used in our tests are very similar. The only difference is that the RBF interpolation on a sphere using (10) performs slightly better than using (13).

Using all the previous results we can choose the best shape parameter to be $\varepsilon = 4$ for $5 \cdot 10^3$ and 10^4 sampling points and $\varepsilon = 2$ for 10^3 sampling points. For this parameters the interpolation errors are the smallest, the RBF interpolation matrix is sparse and has a rather small condition number. For $\varepsilon > 4$, resp. $\varepsilon > 2$, will increase both interpolation errors and for $\varepsilon < 4$, resp. $\varepsilon > 2$, will increase the occupancy and the condition number of RBF interpolation matrix.

The RBF interpolated vector field (8) on a unit sphere was visualized using the line integral convolution, see Figure 3. The important property of the interpolated vector field is that for all shape parameters $\varepsilon < 4$ it preserves the type of all critical points in the vector field (8). And the location of all critical points in the interpolated vector field is almost identical to the locations of the critical points in the vector field (8). Thus the RBF interpolated vector field has the same topology as the vector field (8).

V. CONCLUSION

We presented an approach for vector field interpolation using radial basis functions on a sphere. The distance between two points is computed over the surface, as it is more natural and the interpolation is more accurate. The presented experiments showed how the interpolation error, the matrix occupancy, and the condition number of the interpolation matrix depends on the value of the shape parameter of the RBF.

VI. ACKNOWLEDGMENTS

The authors would like to thank their colleagues at the University of West Bohemia, Plzen, for their discussions and suggestions, and the anonymous reviewers for their valuable comments and hints provided. The research was supported by MSMT CR projects LH12181, SGS 2016-013 and GA17-05534S.

VII. REFERENCES

[1] Aguilar, F. J., et al. Effects of terrain morphology, sampling density, and interpolation methods on grid DEM accuracy. Photogrammetric Engineering & Remote Sensing, Vol. 71, No. 7, pp. 805-816, 2005.

[2] Baxter, B. J., Hubbert, S. Radial basis functions for the sphere. Recent Progress in Multivariate Approximation, pp. 33-47, Birkhäuser Basel, 2001.

[3] Eldrandaly, K. A., Abu-Zaid, M. S. Comparison of Six GIS-Based Spatial Interpolation Methods for Estimating Air Temperature in Western Saudi Arabia. Journal of environmental Informatics, Vol. 18, No. 1, 2011.

[4] Flyer, N. et al. Radial basis function-generated finite differences: A mesh-free method for computational geosciences. Handbook of Geomathematics. Springer, Berlin, 2014.

[5] Golitschek, M. V., Light, W. A. Interpolation by polynomials and radial basis functions on spheres. Constructive Approximation, Vol. 17, No. 1, pp. 1-18, 2001.

[6] Günther, T., Theisel, H. Inertial Steady 2D Vector Field Topology, Computer Graphics Forum (Proc. Eurographics), Vol. 35, No. 2, 2016.

[7] Hardy, R. L. Multiquadric equations of topography and other irregular surfaces. Journal of geophysical research, Vol. 76, No. 8, pp. 1905-1915, 1971.

[8] Hubbert, S., Lê Gia, Q. T., Morton, T. M. Spherical radial basis functions, theory and applications. ISBN: 978-3-319-17938-4, Springer, 2015.

[9] Wendland, H.: Piecewise polynomial, positive definite and compactly supported radial functions of minimal degree. Advances in computational Mathematics, Vol. 4, No. 1, pp. 389-396, 1995.

[10] Zanino, R., et al. Computational Fluid Dynamics (CFD) analysis of the Helium inlet mock-up for the ITER TF superconducting magnets. Applied Superconductivity, IEEE Transactions on, Vol. 24, No. 3, pp. 1-5, 2014.